Molecular Crystals and Liquid Crystals Science and Technology. Section A. Molecular Crystals and Liquid Crystals

Publication details, including instructions for authors and subscription information:
http://www.tandfonline.com/loi/gmcl19

Phase Diagram of Confined Antiferroelectric Liquid Crystals in an Electric Field

Tiezheng Qian [a] & P. L. Taylor [a]

[a] Department of Physics, Case Western Reserve University, Cleveland, Ohio, 44106, USA

Version of record first published: 24 Sep 2006

To cite this article: Tiezheng Qian & P. L. Taylor (2000): Phase Diagram of Confined Antiferroelectric Liquid Crystals in an Electric Field, Molecular Crystals and Liquid Crystals Science and Technology. Section A. Molecular Crystals and Liquid Crystals, 351:1, 229-236

To link to this article: http://dx.doi.org/10.1080/10587250008023272

Mol. Cryst. and Liq. Cryst., 2000, Vol. 351, pp. 229-236
Reprints available directly from the publisher
Photocopying permitted by license only

Phase Diagram of Confined Antiferroelectric Liquid Crystals in an Electric Field

TIEZHENG QIAN and P. L. TAYLOR

Department of Physics, Case Western Reserve University, Cleveland, Ohio 44106, USA

We study the electric-field-induced transitions in antiferroelectric liquid crystals in a model that takes into account the intralayer elastic distortion, the nearest-neighbor interlayer interaction, the coupling of the spontaneous polarization with the applied field, the dielectric anisotropy, and the surface anchoring. We find that the field-induced phase sequence has a critical dependence on cell thickness. For moderately thin cells (thickness > 0.1 μm) with moderately strong anchoring (surface coupling ~ 10^{-4} J/m^2), the system, in departing from the initial anticlinic alignment, first undergoes a continuous Fréederiksz transition, then a first-order surface boundary-layer transition, and finally a first-order or continuous transition to a complete synclinic ordering. Reducing the cell thickness to less than 0.1 μm will make the Fréedericksz transition and even the boundary-layer transition vanish.

Keywords: antiferroelectric liquid crystal; phase diagram

INTRODUCTION

Since the discovery of antiferroelectricity in smectic C^* liquid crystals [1], there has been considerable interest in the electric-field—induced transition between antiferroelectric (AF) smectic C^*_A (SC^*_A) and ferroelectric (F) smectic C^* (SC^*) phases in AF liquid crystals (AFLCs), because

tristable switching has shown great advantages over the bistable switching found in surface-stabilized ferroelectric liquid crystal (SSFLC) cells in display applications. Various theoretical studies have been carried out to investigate the static and dynamic aspects of the field-induced effects in bulk AFLCs [2] and AFLC cells [3].

A simple model based on nearest-neighbor interaction between smectic layers has been proposed as a basis for the study of the various static and dynamic properties of AFLCs [4]. This model takes into account the intralayer elastic distortion, the interlayer interaction, the coupling of local polarization with applied field, the dielectric anisotropy, and the surface anchoring effect. In the present paper, this model is adopted to investigate systematically the field-induced phase transitions in different cell-thickness regimes.

MODEL

The geometry of the system is defined as in Fig. 1. The smectic layers lie in the xz plane and the cell surfaces lie in the xy plane, so that the applied electric field $\mathbf{E}$ is in the z direction. The director $\mathbf{n}$ in the i^{th} layer is assumed to be confined to a cone whose surface is at an angle θ to the layer normal, and is thus completely defined by the azimuthal angle ϕ_i that the projection of $\mathbf{n}$ onto the xz plane makes with the x axis. The electric polarization within a layer is assumed to be of magnitude P_0 and to lie in a direction parallel to $\mathbf{n} \times \hat{\mathbf{y}}$. The local energy density of the interaction of this polarization with an applied electric field is then $-P_0 E \cos\phi_i$. Here we ignore the x-dependence of ϕ.

The working model for the bulk free energy $\mathcal{F}$ of the system is $\mathcal{F} = D\Sigma_i \int f_i dx dz$ [4], with D the layer thickness and f_i the bulk free energy density, given by

$$\begin{aligned} f_i = \quad & \frac{1}{2} K \sin^2\theta \left[\left(\frac{\partial \phi_i}{\partial x} \right)^2 + \left(\frac{\partial \phi_i}{\partial z} \right)^2 \right] \\ & + U \cos(\phi_{i+1} - \phi_i) - \frac{J}{2} \cos[2(\phi_{i+1} - \phi_i)] \\ & - P_0 E \cos\phi_i - \frac{\Delta\epsilon\, \epsilon_0 \sin^2\theta}{2} E^2 \sin^2\phi_i, \end{aligned} \tag{1}$$

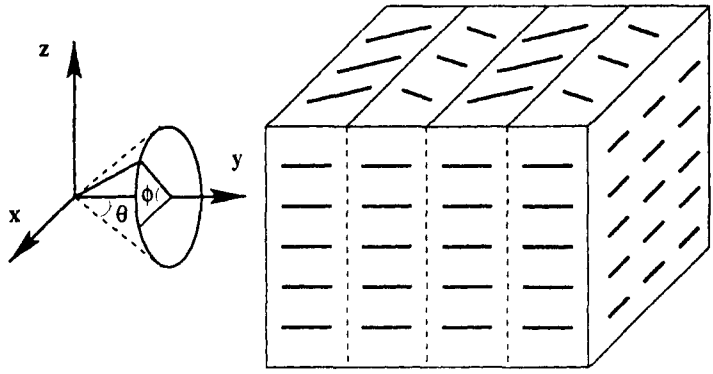

Figure 1: Geometry of the model antiferroelectric liquid crystal.

where K is the effective elastic constant, $U > 0$ and $J > 0$ are interlayer coupling constants, P_0 is the spontaneous polarization, and $\Delta\epsilon$ is the dielectric anisotropy. It is clear that in the right-hand side of Eq. (1), the first term comes from the elastic energy due to the intralayer director distortion, the second two terms represent the interlayer interaction energy, and the last two terms are caused by the applied field through its coupling with the local polarization and the dielectric anisotropy respectively. To account for the surface anchoring effect, we include in the total free energy density a term $w_0[\delta(z+d/2)+\delta(z-d/2)]\sin^2\phi_i$ with d the cell thickness and w_0 a positive constant when the surface anchoring is planar. For polar anchoring, a further term $w_1[\delta(z+d/2)-\delta(z-d/2)]\cos\phi_i$ must be added, but we neglect this complication in favor of a model of non-polar anchoring.

In the AF phase in the absence of an applied field, the angles ϕ_i alternate between 0 and π as one passes from layer to layer. We assume that with our neglect of helicity, this pattern of alternation persists in the presence of applied fields. We then need consider only the values of $\phi_i(z)$ within two adjacent layers. All succeeding pairs of layers will then merely be a repetition of these. We denote the value of ϕ_i in all odd layers as φ and in all even layers as $\pi+\psi$. At equilibrium in the field-free AF structure we then have $\varphi = \psi = 0$.

EQUILIBRIUM STATES AND PHASE TRANSITIONS

Numerical calculations were carried out using the full expression for the free energy. We use a finite difference scheme to discretize the free energy functional and employ the quasi-Newtonian method to seek the optimal configurations. The equilibrium state is given by those values of $\phi(z)$ and $\psi(z)$ that minimize the free-energy functional. Close to the (first-order) transition point, the continuation method was used to obtain the desired state. In this way, global optimal configuration in one regime may be used to obtain the metastable (locally optimal) configuration in other regimes. We note that the ultra-thin cells to which part of this analysis is applicable have not yet been reliably manufactured.

Moderately Thin Cells

For moderately thin cells ($d > 0.1$ μm), the unperturbed AF state becomes unstable when the applied field is sufficiently large. This is due to the competition between the bulk field-induced free energy which is minimized at $\phi+\psi = \pi$ and the surface-to-bulk elastic distortion energy which is maximized if the bulk $\phi + \psi$ equals to π. The continuous Fréedericksz transition occurs when the unperturbed AF state becomes absolutely unstable. After that, the bulk values of ϕ and ψ both increase from zero towards $\pi/2$ (see Fig. 2), accompanied by a much slower increase of the surface values of ϕ and ψ. Increasing the field will eventually break the surface anchoring, resulting in a first-order surface boundary-layer transition with surface ϕ and ψ jumping away from the old orientations that are close to the easy axes. Meanwhile, if the cell thickness is relatively small, the bulk angles can also experience their own jump at the surface transition (see Fig. 2-(b)). Further increasing the field will make the ideal F state ($\phi(z) = 0$ and $\psi(z) = \pi$ for $-d/2 \leq z \leq d/2$), which minimizes the field energy and the elastic energy simultaneously, the new equilibrium state, therefore leading to an AF-F transition. In the thick cell regime ($d > 1$ μm), we find that this transition can be either first-order or second-order, depending on the values of certain model parameters.

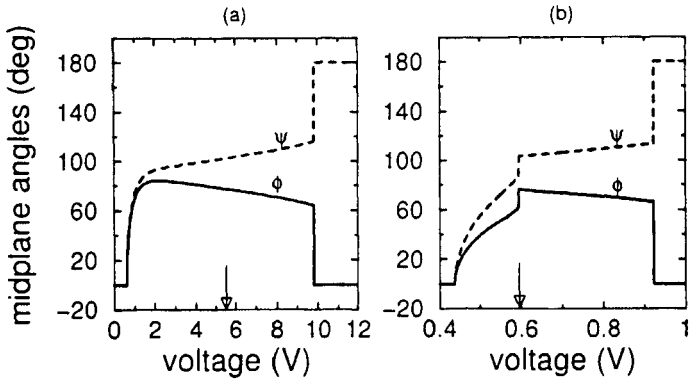

Figure 2: The midplane director orientations ϕ (solid line) and ψ (dashed line) of alternate smectic layers are plotted as functions of applied voltage. (a) $d = 1$ μm. (b) $d = 0.1$ μm. The location of the surface boundary-layer transition is marked by the downward arrow. The parameters defined in the text used for calculation are $K = 10^{-11}$ N, $U = 3.0 \times 10^3$ J/m^3, $J = 1.0 \times 10^3$ J/m^3, $P_0 = 7.5 \times 10^{-4}$ C/m^2, $\Delta\epsilon = -1.0$, $\theta = 20°$, and $w_0 = 1.0 \times 10^{-4}$ J/m^2.

Extremely Thin Cells

For extremely thin cells ($d < 0.1$ μm), the phase sequence is quite different (see Fig. 3). The underlying physics is not difficult to understand. Basically, there are four length scales in determining the qualitative behavior of the phase sequence. They are: (1) the intrinsic AF correlation length

$$\xi_{AF} = \sqrt{K \sin^2\theta / 4U},$$

(2) the field-induced correlation length

$$\xi_E = \sqrt{4(U + 2J) K \sin^2\theta / P_0^2 E^2},$$

(3) the surface extrapolation length

$$l = K \sin^2\theta / w_0,$$

(here $l > \xi_{AF}$), and (4) the cell thickness d. For $d >> l$, the Fréedericksz transition occurs first when $\xi_E \sim d$ and the surface breaking then occurs

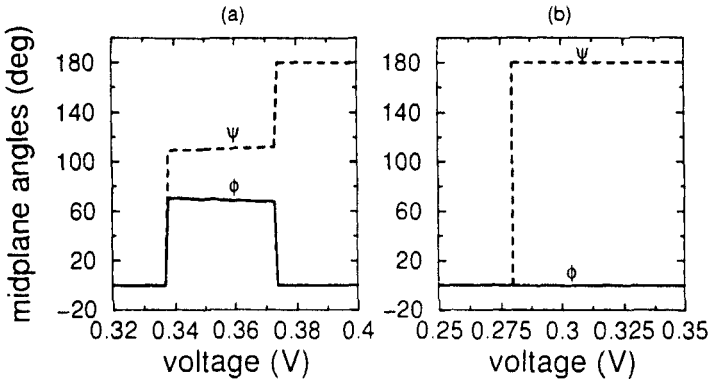

Figure 3: The midplane director orientations ϕ (solid line) and ψ (dashed line) of alternate smectic layers are plotted as functions of applied voltage. (a) $d = 0.045$ μm. (b) $d = 0.035$ μm. Other parameters used for calculation are the same as those for Fig. 2.

when $\xi_E \sim l$. But if $d \sim l$ or $d < l$ (see Fig. 3-(a)), then the surface transition precedes the Fréedericksz transition which will never occur. As a result, the surface and the bulk angles undergo their abrupt changes simultaneously at the surface transition. After that, the AF-F transition occurs when $\xi_E \sim \xi_{AF}$. In the case $d \sim \xi_{AF}$ or $d < \xi_{AF}$ (see Fig. 3-(b)), the severe confinement condition prevents any spatial variation of the partial AF ordering across the cell from being stabilized. In consequence, the only transition left is the one between the unperturbed AF state and the ideal F state.

PHASE DIAGRAM

The phase diagram of AFLC cells is depicted in Fig. 4. It is seen that for all but the thinnest cells ($d > 0.1$ μm), there are three successive transitions, i.e., the continuous Fréedericksz transition, the first-order surface boundary-layer transition, and the AF-F transition (of first-order for the parameters used in calculating the present phase diagram). That is, the Fréedericksz transition first transforms the system from the unperturbed AF state into the bulk-rotated AF (BRAF) state which exhibits

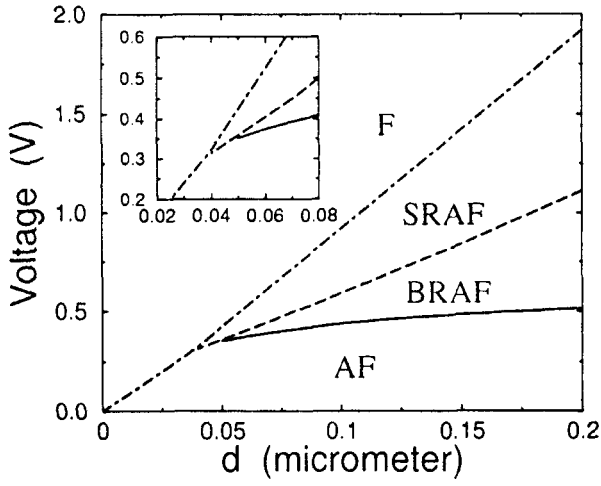

Figure 4: Phase diagram of the alignment state in antiferroelectric liquid crystal cells. The inset provides the detail around $d = 0.05$ μm. Here $w_0 = 0.6 \times 10^{-4}$ J/m^2, and the parameters K, U, J, P_0, $\Delta\epsilon$ and θ are the same as those used for Fig. 2.

small deviation of the surface directors from the easy axes. The surface boundary-layer transition then transforms the system from the BRAF state into the surface-rotated AF (SRAF) state in which the surface anchoring is broken and thus the surface-to-bulk elastic distortion energy lowered. The system finally goes into the ideal F state through the AF-F transition. If we let V_F, V_s, and V_{th} denote the critical voltages for the Fréedericksz transition, the surface boundary-layer transition, and the AF-F transition, respectively, then in the limit of $d \to \infty$, we have V_F independent of d, $V_s \propto d$, and $V_F \propto d$. Reducing the cell thickness to less than 0.1 μm $\sim l$ will first terminate the existence of the Fréedericksz transition. Consequently, the system is transformed directly from the unperturbed AF state into the SRAF state through a first-order transition which comprises the simultaneous rotations of the surface and the bulk directors. The AF-F transition then occurs as in moderately thin cells. Further reducing the cell thickness leads to a direct transformation

from the unperturbed AF state into the ideal F state at $V_{th} = 2Ud/P_0$, with no intermediate state.

SUMMARY

We have studied the field-induced transitions in a model that takes into account the intralayer elastic distortion, the nearest-neighbor interlayer interaction, the coupling of spontaneous polarization with applied field, the dielectric anisotropy, and the surface anchoring. We find that the AFLC cells show qualitatively different phase sequences in different cell thickness regimes. The study of the corresponding dynamical behavior of such AFLC cells is being undertaken.

Acknowledgments

We thank C. Rosenblatt, X. Y. Wang, and S. Zhang for helpful discussions. This work was supported by the National Science Foundation Science and Technology Center for Advanced Liquid Crystalline Optical Materials (ALCOM) through Grant No. DMR89-20147.

References

[1] A.D.L. Chandani, T. Hagiwara, Y. Suzuki, Y. Ouchi, H. Takezoe, and A. Fukuda, *Jpn. J. App. Phys.* **27**, L729 (1988); A.D.L. Chandani, E. Gorecka, Y. Ouchi, H. Takezoe, and A. Fukuda, *Jpn. J. App. Phys.* **28,** L1265 (1989).

[2] H. Sun, H. Orihara, and Y. Ishibashi, *J. Phys. Soc. Jpn.* **62,** 2706 (1993); B. Zeks and M. Cepic, *Liq. Cryst.* **14**, 445 (1993); A. Roy and N.V. Madhusudana, *Europhys. Lett.* **36,** 221 (1996).

[3] M. Nakagawa, *Jpn. J. App. Phys.* **30,** 1759 (1991); T. Akahane and A. Obinata, *Liq. Cryst.* **15,** 883 (1993); M. Nakagawa, *Liq. Cryst.* **14,** 1763 (1993).

[4] J.F. Li, X.Y. Wang, E. Kangas, P.L. Taylor, C. Rosenblatt, Y. Suzuki, and P.E. Cladis, *Phys. Rev. B* **52,** R13075 (1995); X.Y. Wang and P.L. Taylor, *Phys. Rev. Lett.* **76,** 640 (1996); X.Y. Wang, T. Kyu, A.M. Rudin, and P.L. Taylor, *Phys. Rev. E* **58,** 5919 (1998); X.Y. Wang. J.F. Li, E. Gurarie, S. Fan, T. Kyu, M.E. Neubert, S.S. Keast, and C. Rosenblatt, *Phys. Rev. Lett.* **80,** 4478 (1998).